Radiología. 2020;62(2):90–101

RADIOLOGÍA

www.elsevier.es/rx

UPDATE IN RADIOLOGY

Update in the evaluation of peripheral nerves by MRI, from morphological to functional neurography☆

T. Martín Noguerol[a,*], **R. Barousse**[b]

[a] *Sección de Neurorradiología, Clínica las Nieves, HT SERCOSA, Jaén, Spain*
[b] *Departamento de nervio periférico y plexos, Centro Rossi, Buenos Aires, Argentina*

Received 24 January 2019; accepted 24 June 2019

KEYWORDS
Magnetic resonance imaging;
Diffusion;
Diffusion tensor imaging;
Peripheral nerve

Abstract Imaging studies of peripheral nerves have increased considerably in the last ten years. In addition to the classical and still valid study by ultrasound, new neurographic techniques developed from conventional morphological sequences (including 3D isotropic studies with fat suppression) are making it possible to assess different peripheral nerves and plexuses, including small sensory and/or motor branches, with great precision. Diffusion-weighted sequences and diffusion tensor imaging have opened a new horizon in neurographic studies. This new approach provides morphological and functional information about the internal structure and pathophysiology of the peripheral nerves and diseases that involve them. This update reviews the different MR neurography techniques available for the study of the peripheral nerves, with special emphasis on new sequences based on diffusion.

PALABRAS CLAVE
Resonancia magnética;
Difusión;
Tensor de difusión;
Nervio periférico

Actualización en la valoración de los nervios periféricos mediante resonancia magnética: de la neurografía morfológica a la funcional

Resumen El estudio los nervios periféricos (NNPP) mediante técnicas de imagen ha experimentado un notable crecimiento en la última década. Más allá del abordaje clásico y todavía vigente mediante ecografía de los NNPP, el desarrollo de nuevas técnicas neurográficas a partir de secuencias morfológicas convencionales (incluyendo estudios 3D isotrópicos con supresión

☆ Please cite this article as: Martín Noguerol T, Barousse R. Actualización en la valoración de los nervios periféricos mediante resonancia magnética: de la neurografía morfológica a la funcional. Radiología. 2020;62:90–101.

* Corresponding author.
E-mail address: t.martin.f@htime.org (T. Martín Noguerol).

grasa) está permitiendo valorar los distintos NNPP y plexos incluyendo pequeñas ramas terminales sensitivas y/o motoras con gran precisión. El uso de secuencias potenciadas en difusión (DWI) y tensor de difusión (DTI) ha permitido abrir un nuevo horizonte en los estudios de neurografía. Este nuevo abordaje proporciona información morfológica y funcional acerca de la estructura interna y fisiopatología de los NNPP y las distintas patologías relacionadas con ellos. En esta actualización realizamos una puesta al día de las distintas modalidades de neurografía mediante resonancia magnética disponibles para el estudio de los NNPP, con especial atención a las nuevas secuencias basadas en difusión.

Introduction

Considerable advances have been made in the study of peripheral nerves, brachial and lumbar plexuses using imaging techniques in recent years, thanks to the development of specific neurographic imaging techniques.[1] Until recently, nerve conduction inside peripheral nerves could only be evaluated by performing neurophysiology studies, mainly electroneurography and electromyography. These techniques are still valid today, and are very useful for studying neuropathies; however, they are invasive, and can be prone to considerable intersubject variability.[2] Peripheral nerves can be evaluated using different imaging techniques, such as ultrasound, computed tomography (CT) or magnetic resonance imaging (MRI). The main characteristics of these techniques are summarised in Table 1.[3] In the case of CT, the low contrast resolution of this technique, together with the inherent use of ionising radiation, limits its use to very specific situations, such as assessing the relationship between peripheral nerves and bone structures, and studying peripheral nerve calcifications or muscle fat infiltration.[4] For this reason, the imaging techniques of choice for studying peripheral nerves are ultrasound and MRI. The main advantages of ultrasound are its accessibility, spatial resolution, and its ability to provide real-time, dynamic data by performing certain bodily movements.[5] One of the main limitations of ultrasound is its high dependence on operator training and experience, which can increase the rate of false negatives and false positives.[3] In addition, many peripheral nerves are located deep in the body, or adjacent to bone structures or abdominal viscera such as the lumbar plexus, making it difficult to evaluate them accurately using ultrasound.

The introduction of MRI to evaluate normal and pathological peripheral nerves gives higher sensitivity and specificity in different clinical scenarios, in many of which it improves the benefits hitherto offered by conventional techniques.[6] With the introduction of magnetic resonance neurography (MRN) (which identifies and visualises, both selectively and non-selectively, peripheral nerve pathways and morphological or functional characteristics), radiologists can now obtain high-resolution images of peripheral nerves, regardless of their anatomical location. These images show the morphological and pathological characteristics of peripheral nerves in great detail, and are very useful in the study of peripheral neuropathies.[7–9] The development of new, advanced MRN techniques has allowed radiologists to progress from a morphological, qualitative assessment to a functional, quantitative assessment of peripheral nerves and peripheral nerve plexuses.[10] This has been made possible by functional MRI sequences based on diffusion-weighted imaging (DWI) and diffusion tensor imaging (DTI).[11] These techniques have been applied in recent decades with excellent results, particularly in the evaluation of ischaemic and tumour pathology in the central nervous system.[12] The extrapolation of these peripheral nerve study techniques presents both a technical and diagnostic challenge, since the signs and parameters obtained from the images must be evaluated in the clinical context and anatomical characteristics of each region to be studied.

In this article, we will describe the latest types of morphological and functional sequences, selective and non-selective, for the assessment of peripheral nerves. We will also update the potential clinical uses of MRN in terms of evaluating not only the morphology, but also the pathophysiology of peripheral nerves and peripheral nerve plexuses.

Morphological MRN

The evaluation of peripheral nerves using non-selective or selective MRI sequences is called magnetic resonance neurography. Non-selective MRN sequences are those that show not only the peripheral nerves but also bone or muscle structures. To obtain selective sequences, different technical adjustments are made that eliminate the background structures and/or enhance the signal of the peripheral nerves to make them more easily identifiable.[1]

These studies are based on conventional T1- and T2-weighted sequences, with some technical peculiarities. Isotropic voxel acquisitions make it possible to obtain 3 D images that can be reconstructed in different planes, including oblique or curved planes.[13] This makes it possible to identify peripheral nerve pathways, even in complex anatomical regions, such as the osteotendinous plexuses or outlets.[14] T1-weighted sequences provide a great deal of detail about the structure of the nerve, since their high resolution can delimit the different nerve fascicles,

Table 1 Imaging techniques for the evaluation of peripheral nerves.

	CT	Ultrasound	MRI
Spatial resolution	Good	Excellent	Very good
Contrast resolution	Poor	Good	Excellent
Dynamic data	No	Yes	No
Functional data	No	No	Yes (DWI and DTI)
Reconstruction	Multiplanar	No	Multiplanar
Ionising radiation	Yes	No	No
Operator-dependence	Low	Maximum	High
Muscle evaluation	Limited	Moderate	Optimal
Availability	Widely available	Widely available	Limited

DTI: diffusion tensor imaging; DWI: diffusion-weighted imaging.

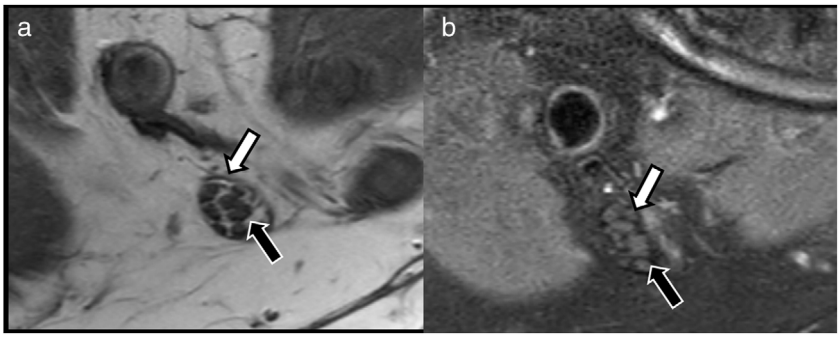

Figure 1 Evaluation of peripheral nerve structure using conventional neurography sequences. A) Axial T1-weighted TSE image. B) T2-weighted SPAIR fat suppression image of the tibial nerve in the popliteal hollow, showing preserved fascicular pattern that is easily evaluated due to the connective and fatty tissue that separates the endoneurium from the perineurium (black arrow) and epineurium (white arrow).

and distinguish between the endoneurium, perineurium and epineurium, which often contain thin layers of connective tissue and fat (Fig. 1). In the last decade, the acquisition of high-resolution T2-weighted images with isotropic voxels and fat-suppression techniques has improved the anatomical resolution of peripheral nerves and heightened the contrast with the adjacent structures.[10] These fat suppression pulses are usually performed using SPAIR or 3 D SPIR sequences, which have a good signal/noise ratio; however, they also suppress fat located far from the isocentre of acquisition due to the lower homogeneity of the magnetic field. This can be resolved by using fat suppression sequences based on Dixon techniques which, being less sensitive to the heterogeneities of the magnetic field, obtain more homogeneous fat suppression. Dixon techniques also obtain four sets of images with a single acquisition (in-phase, out-of-phase, water only and fat only), thus reducing the time needed to complete the scan.

Other technical optimisations, such as the use of multichannel coils, coils tailored to the anatomy of the area to be studied (including surface coils), have improved image quality by obtaining high-resolution isotropic sequences. The use of parallel acquisition techniques, in 1.5 T or, in particular, 3.0 T scanners, can also be used to reduce scan time and even increase the signal-to-noise ratio of the acquisitions and reduce the risk of artefacts.

The use of specific pulses to suppress the signal inside the vessels or the application of diffusion gradients with low *b* values (50 s/mm^2) is part of a new range of technically optimised sequences for selective evaluation of peripheral nerves.[15] These sequences facilitate visualisation of the peripheral nerves by reducing the possibility of false positives due to the presence of adjacent vascular structures (Fig. 2). In the case of morphological MRN, gadolinium is only used in special circumstances in which infection or inflammation is suspected, or when the scan is performed for tumour characterisation.[3] In these patients, rupture of the blood-nerve barrier will result in pathological uptake. The imaging appearance and differentiating factors of tumours associated with peripheral nerves have also been described in detail, including schwannomas, neurofibromas and malignant tumours of the neural sheath, or pseudotumours such as neuromas. Identification is based on the degree of displacement of the nerve fascicles or preservation of fat planes with adjacent structures.[16]

The appearance of pathological peripheral nerves in MRN studies may vary, depending on different clinical scenarios (compression, traction, section, inflammation and infiltration). As a general rule, a pathological peripheral nerve will have a larger diameter and a higher signal intensity in T2-weighted sequences, which will become more apparent if fat suppression pulses are applied. This increase in signal intensity and nerve volume can be easily evaluated when compared with other adjacent nerves or even with the vascular bundle (artery and vein) that usually accompany the nerve of interest, and that can serve as an internal

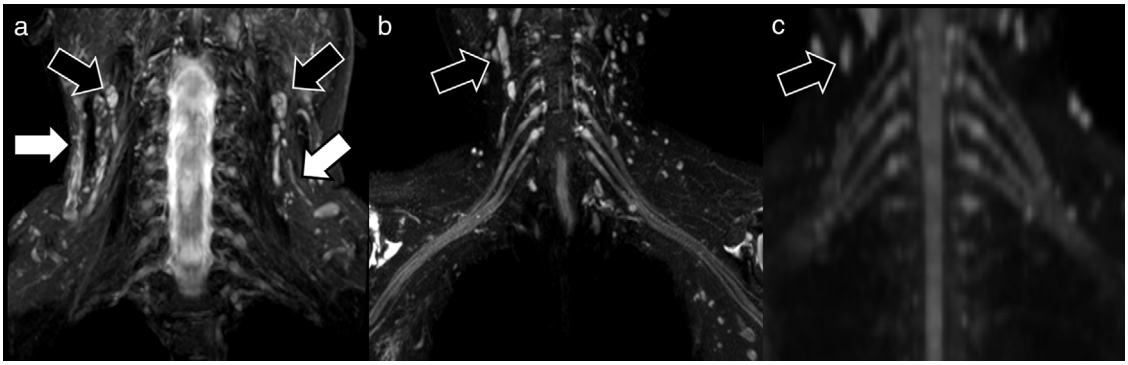

Figure 2 Examples of neurographic techniques for evaluating the brachial plexus. The morphological sequences obtained using fat suppression (A), coronal STIR in this case, show the trunks and roots of the brachial plexus. The image, however, is not selective, since other structures such as muscles, blood vessels (white arrows), bone or lymph nodes (black arrows) are also visible. In the case of hybrid techniques, such as 3D Nerve View (coronal plane) (B), the use of selective pulses to suppress the signal from blood vessels (main source of false positives) gives a more accurate assessment of the nerves; however, it does not eliminate other structures, such as lymph nodes (black arrows). Functional selective sequences, DWI with coronal multiplanar reconstruction (C), show the peripheral nerves almost exclusively (with the exception of some lymph nodes [black arrows], which also show normal diffusion restriction in the axial plane) with good suppression of the background signal.

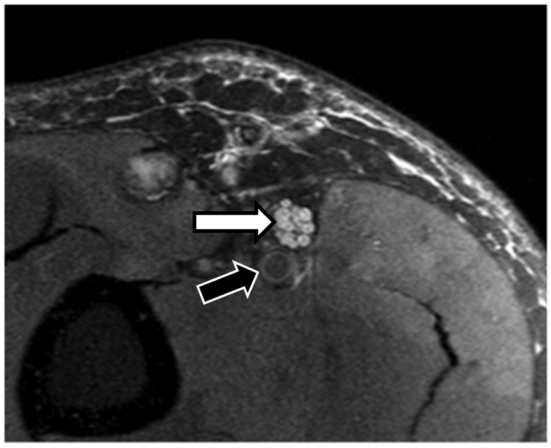

Figure 3 A 38-year-old man who presented with paraesthesia in the territory of the left median nerve. An axial proton density (PD) SPAIR sequence showing fascicular thickening of the median nerve (white arrow). There is an increase in the volume and intensity of the nerve signal with respect to the adjacent vessel (black arrow), compatible with neuritis, and diagnosed as nonspecific vasculitis on biopsy.

reference.[17] In the case of the sciatic nerve, for example, an increase in the nerve-to-vessel diameter ratio of over 0.89 should be considered pathological.[18] This increase in signal intensity and diameter is mainly due to an increase in the volume of water between the different nerve fascicles as a result of venous congestion, oedema, ischaemia, and ultimately, Wallerian degeneration changes[19] (Fig. 3).

Variations in the expected anatomical location of each peripheral nerve, or the presence of adhesions with adjacent osteotendinous structures, should raise suspicion of peripheral nerve pathology.[20] In the case of neural injury, Seddon and later Sunderland classified the type of neural damage on the basis of the extent of peripheral nerve involvement.[21,22] For example, the mildest degree of involvement is neurapraxia (grade I), which is identified by a discrete alteration in peripheral nerve signal intensity in T2-enhanced sequences (with and without fat suppression). Next comes axonotmesis, which involves axonal damage with probable changes due to Wallerian degeneration, although the peripheral nerve is preserved. According to Sunderland, axonotmesis can be subdivided into three stages, depending on whether the damaged structure corresponds to the axon (grade II), the endoneurium (grade III) or the perineurium (grade IV). And finally, there is neurotmesis, in which the peripheral nerve is severed, usually due to dissection or traction of the nerve, with damage of the epineurium (grade V).[23] Grade IV and V injuries usually require surgery.

A secondary sign that usually accompanies pathological peripheral nerves is the existence of muscular denervation (acute, subacute or chronic) due to changes in signal intensity in the distal muscle groups dependent on the nerve, particularly in cases of mixed sensory and motor injury[24] (Fig. 4). MRN mapping of muscular denervation can often indicate the type of peripheral nerve affected.

Functional diffusion-based MRN

This is a type of selective MRN, and is based on the use of DWI and DTI sequences. DWI sequences are capable of assessing and quantifying, *in vivo*, the movement of water molecules inside biological structures. Water diffusion can be restricted to a greater or lesser extent by the presence of biological barriers (membranes) or by an increase or decrease in extracellular space.[12]

Diffusion-based techniques are suitable for evaluating both the macro and microscopic structure of peripheral nerves. Peripheral nerves present a highly organised structure with numerous barriers, such as the epineurium, the perineurium and the endoneurium. These layers, together with the myelin sheaths that surround the axons, determine the two types of movement within peripheral nerves. The first takes place along the short (perpendicular) axis

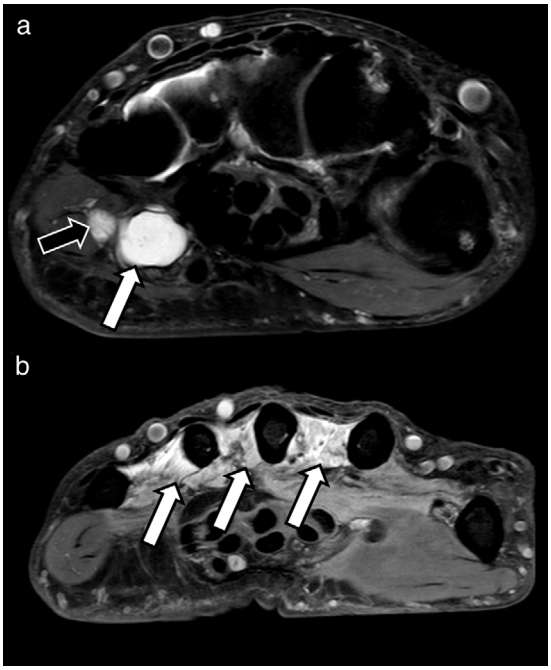

Figure 4 Extrinsic compression of the ulnar nerve in a 32-year-old man with loss of strength in the fingers of the right hand lasting several months. A) The PD SPAIR sequence shows a ganglion lesion (white arrow) at the entrance of the Guyon canal impinging on the ulnar nerve (black arrow), which is thickened and hyperintense, suggesting extrinsic compression neurapraxia. B) The same study showing extensive alteration of the signal intensity of the lumbar muscles (white arrows), compatible with changes due to subacute muscle denervation.

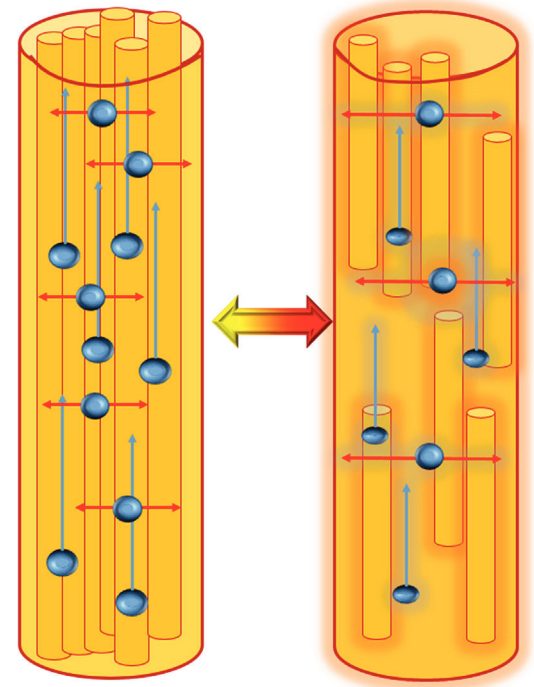

Figure 5 Behaviour of water molecules inside the peripheral nerves. In a *normal peripheral nerve*, the presence of physiological barriers, such as the myelin sheath and the layered structure of the peripheral nerves, limits the movement of water in the axial plane (transverse, red arrows), thus allowing them to be studied using standard DWI sequences that show normal diffusion restriction in that plane. In addition, water molecules also move along the major axis of the peripheral nerves (blue arrows). This dominant (anisotropic) diffusion along the major axis of the nerve allows these structures to be studied using DTI sequences.
In a *pathological peripheral nerve*, the existence of intrinsic or extrinsic damage in the structure of the nerve will lead to oedema, with an increase in the extracellular space, or loss of myelin. In this case, water diffusion in the axial plane will increase (red arrows), and will be shown as an increase in apparent diffusion coefficient (ADC)/average diffusivity and radial diffusivity (RD) values, as well as a decrease in the level of axonal organisation, which will be shown by a decrease in fractional anisotropy (FA) values. This process can be reversible if the neural damage is repaired, and will be shown by normalisation of the aforementioned values, in other words, increase in FA and decrease in ADC/mean diffusivity and radial diffusivity values.

of the nerve, where the movement of water molecules is highly limited due to the existence of the aforementioned physiological barriers. This movement, known as isotropic diffusion, can be studied by conventional DWI sequences that are capable of detecting limited water movement in the axial plane.[25]

In the second type of movement, water moves along the axons and the major axis of the nerve. This type of movement is known as anisotropic diffusion, in which the water molecules are displaced in a single, dominant direction. It is mainly this property that allows DTI to identify peripheral nerves using the same technique applied to the study of white matter tracts in the central nervous system. DTI allows 3 D visualisation of peripheral nerves, showing both their relationship with adjacent structures and their intrinsic and extrinsic lesions[26] (Fig. 5).

As far as the technical specifications are concerned, DWI-neurography sequencing is based on the classic single-shot echo-planar imaging (EPI). In the case of diffusion-based neurography, most studies recommend acquiring maximum *b* values of between 600 and 800 s/mm^2.[7,27] This will identify the peripheral nerves, plexus roots or trunks while suppressing the background signal of other structures. However, signal intensity in DWI sequences is increased in some normal structures in certain anatomical areas, such as the neck or pelvis; these include lymph nodes, attachments or slow-flow vessels such as pelvic varicose veins. Therefore, careful postprocessing using multiplanar reconstruction (MPR) techniques is essential to differentiate between both structures, taking as a reference the morphological image.[28]

With regard to DTI studies, which are also based on single shot EPI acquisitions, maximum *b* values of 600—800 s/mm^2 and between six and 32 directions should be used. This sequence is more sensitive to the heterogeneities of the magnetic field, which are accentuated in the assessment of certain anatomical areas such as the brachial plexus due to the existence of multiple interfaces between water, fat, bone and air. As such, they make it difficult to obtain functional neurography studies with adequate diagnostic quality.

Table 2 DTI-derived parameters for the evaluation of peripheral nerves.

	Fractional anisotropy (FA)	Mean diffusivity (MD)	Axial diffusivity (AD)	Radial diffusivity (RD)
Units	0-1	mm^2/s	mm^2/s	mm^2/s
Formula	$\sqrt{\frac{1}{2}}\frac{\sqrt{(\lambda_1-\lambda_2)^2+(\lambda_2-\lambda_3)^2+(\lambda_3-\lambda_1)^2}}{\sqrt{\lambda_1^2+\lambda_2^2+\lambda_3^2}}$	$\frac{\lambda_1+\lambda_2+\lambda_3}{3}$	$\lambda_1 = \lambda_{\parallel}$	$\lambda_1 = {}^{(\lambda_2+\lambda_3)}/_2$
Evaluation	Fascicular organisation	Extracellular compartment	Axonal integrity	Myelin Integrity

ADC: apparent diffusion coefficient; DTI: diffusion tensor imaging; λ_1: main eigenvalue; λ_2 λ_3: minor eigenvalues.

When deciding whether to perform DWI or DTI, certain factors must be taken into account. DWI neurography can give a large field of view with a short acquisition time and with good background signal suppression. DTI studies take longer, so they should only be used, *a priori*, for targeted studies in specific, smaller, anatomical areas. DTI studies provide a greater number of parameters with respect to DWI neurography, as described below. As for the type of magnet, as a general rule, studies using 3 T devices will have greater spatial resolution and will require less time than 1.5 T scanners; however, they are more susceptible to artefacts,[27] particularly in anatomical regions where the magnetic field is more heterogeneous, such as in the brachial plexus. As mentioned above, the use of coils specific to the anatomy of the study area, as well as parallel acquisition techniques, will help reduce these artefacts.

In addition to visualising the morphology of peripheral nerves, DWI and DTI neurography sequences also provide a large number of quantifiable parameters. These parameters, which are obtained during post-processing, show different characteristics of the peripheral nerves.

The apparent diffusion coefficient (ADC) is derived from conventional DWI studies. This parameter quantifies the degree of water molecule displacement in the extracellular space; high ADC values reflect increased water content between axons, and can therefore identify peripheral nerve oedema. If, on the contrary, the extracellular space is reduced, either due to fibrosis or cell proliferation, as in the case of peripheral nerve tumours, the ADC values will decrease.[16]

By means of diffusion gradients in multiple spatial directions, DTI studies can identify eigenvectors and calculate their corresponding values (eigenvalues). The combination of these eigenvalues increase the number of quantifiable parameters obtained in comparison with conventional DWI studies. This gives a clearer picture of the pathophysiological characteristics of the peripheral nerves. Table 2 lists these parameters and summarises their main characteristics. Among them, the parameters most widely studied and used in routine clinical practice are fractional anisotropy (FA) and radial diffusivity (RD). FA is the most sensitive marker of loss of fascicular organisation in peripheral nerves, and is diminished in the presence of neural damage. RD is the most specific marker of myelin sheath involvement, which determines the diffusivity of water molecules in the short (transverse, perpendicular or radial) axis of the peripheral nerve. RD will increase in the presence of damage or loss of myelin integrity in the peripheral nerves. Another less widely used parameter is axial diffusivity (AD), which is equivalent to the greatest eigenvalue, and shows axonal conduction along the peripheral nerve. AD will, hypothetically, be diminished distal to the site of the lesion, particularly in patients with grade IV and V peripheral nerve damage according to the Sunderland classification. Finally, mean diffusivity (MD) is a more accurate measure of the extracellular space than ADC, since it is based on all three main eigenvalues. MD will be increased when the extracellular space is increased, such as in the case of oedema, and will decrease in the presence of tumours, because tumour hypercellularity reduces the extracellular space.[27]

In our opinion, caution is needed when using these parameters as cut-off points to differentiate between healthy and pathological peripheral nerves for diagnostic and therapeutic decision-making. Very few studies have been performed to establish the threshold values of these parameters. Parameters derived from the same peripheral nerve or plexus root in the apparently healthy contralateral limb can sometimes be taken as a point of reference. Bear in mind that the values may vary depending on the type of magnet used, the *b* values, or the number of directions acquired.

Clinical applications

The use of both morphology MRN and more advanced DWI and DTI techniques to evaluate peripheral nerve compression or damage, such as the median nerve in carpal tunnel syndrome or other types of nerve entrapment, has increased exponentially in recent years.[29,30] These techniques have also shown promising results in the study of various types of neuropathies, including monitoring post-surgical changes.[27,31] MRN studies can also be used to study tumours, since they facilitate their differential diagnosis.[16] For practical purposes, a basic protocol for an adequate diagnostic approach to these pathologies with both morphological and functional techniques is proposed in Table 3. Some of these parameters may vary or will need to be adjusted, depending on the technical characteristics of each MRI device, in order to obtain interpretable and reproducible results in the evaluation of peripheral nerves.

Compressive and traumatic pathology

The diagnosis of traumatic or compressive damage of the peripheral nerve, including the brachial and lumbar plexus, is usually made using morphological neurographic sequences.[32] However, diffusion-based neurography studies are able to detect functional abnormalities in patients with no relevant findings in conventional morphological studies.[27] As a general rule, the existence of a traumatic or compressive process on a peripheral nerve will result in the disorganisation of its fibre structure, which translates into a

Table 3 Basic neurography protocol and acquisition parameters.

Parameters	T1	T2 PD SPAIR	3D STIR	DWI	DTI
Plane	Axial	Coronal	Axial	Axial	Axial
TR (ms)	633	7,312	2,200	2,179	10,861
TE (ms)	20	24	261	72	95
Thickness (mm)	4	3.5	1	4	4
GAP (mm)	1	1	0	0	0
Voxel (mm)	0.57/0.57/3.91	0.56/0.56/3.50	0.60/0.60/1.00	1.55/1.51/3.00	2.00/2.00/2.00
Fat suppression	No	SPAIR	STIR	SPIR	SPIR
Directions	–	–	–	–	16
b values (s/mm^2)	–	–	–	0 and 800.	0 and 800.
SENSE	No	1.6	3	2	2
NEX	1	1	2	3	2
Acquisition time (min)	2:28	7:00	6:16	2:50	4:50

Figure 6 A 47-year-old man in follow-up for paraesthesia and loss of strength in the territory of the ulnar nerve of the right hand 3 months after blunt force injury to the volar side of the ipsilateral wrist. A) Morphological study using T2-weighted Dixon water-only axial sequences shows signs of subacute/chronic denervation in the lumbrical muscles (black arrows), with interruption of the ulnar nerve pathway and presence of a small end-bulb neuroma in the proximal extremity (white arrow) (B), also visualised on T2-weighted Dixon water-only coronal sequence (C). Diffusion tensor imaging (DTI) (D) neurography study was requested in order to plan surgery and predict response to neurorrhaphy. In addition to showing interruption of the ulnar nerve, DTI neurography can also help evaluate functional integrity of the distal segment (white arrow) in order to predict a favourable response to surgery. The fact that the structure can be visualised on reconstructed DTI neurological images suggests that its fractional anisotropy (FA) values, and therefore its fascicular structure, are preserved, and there are obvious changes in its parameters that would suggest Wallerian degeneration.

decrease in FA values and an increase in RD values.[33] These data can quantify the severity of peripheral nerve damage, and can therefore be used to establish a prognosis, plan the appropriate treatment and monitor its effectiveness.[34] Functional neurographical sequences, in comparison with the morphological techniques used in conventional MRI and electrophysiology studies, can give earlier diagnosis of the type of lesion involved before denervation or other changes can be detected by other neurophysiological imaging or test techniques.[35] However, larger studies are needed to confirm the validity of the parameters derived from DWI and DTI studies as potential biomarkers of neural damage (Fig. 6).

Evaluation of the median nerve in general, and particularly in carpal tunnel syndrome, has always been a challenge for radiologists. Several studies have shown that ultrasound can be a valid tool for preliminary studies, and in many cases can even provide a definitive diagnosis.[36] However, in some patients, despite their symptoms, there is no apparent cause of median nerve compression, even when they are studied using conventional MRI. This is where diffusion-based neurography techniques are showing promising results in diagnosis and post-treatment monitoring.[29,37] Several studies have reported that FA values decrease by up to two standard deviations below normal levels in patients with symptoms compatible with carpal tunnel syndrome. These findings suggest that the physiological fibre structure of the nerve is disrupted due to compression, which in turn increases the extracellular space and axonal disorganisation secondary to oedema and/or congestion.[38] Recent studies, meanwhile, have evaluated the pre- and postoperative variations in FA and ADC in patients undergoing median nerve release surgery, and have shown a progressive increase in

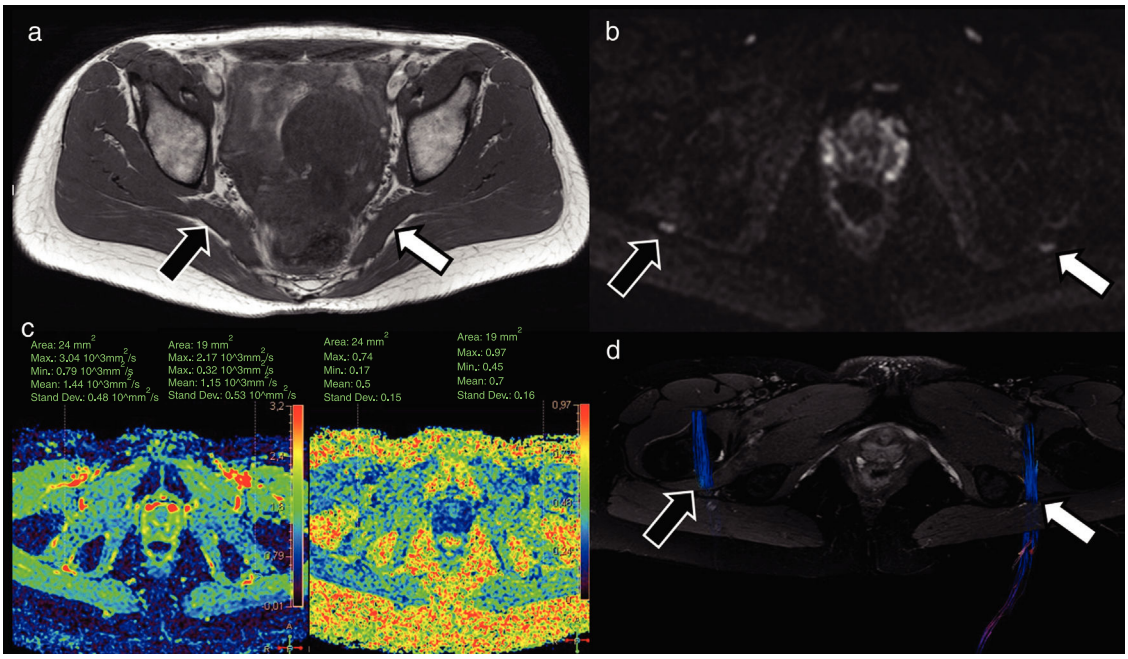

Figure 7 A 41-year-old woman presenting symptoms compatible with right pyramidal syndrome. The axial T1-weighted TSE morphological study (A) shows slight asymmetric thickening of the right pyramidal muscle (black arrow) with respect to the left one (white arrow). The diffusion-weighted sequences (DWI) neurography study (B) identified a slight asymmetric increase in the signal intensity of the right sciatic nerve (black arrow) with respect to the left (white arrow) at the level of the sciatic foramen. The diffusion tensor imaging (DTI) neurographic study (C) showed an increase in the mean diffusivity values of the right sciatic nerve (1.44×10^{-3} mm^2/s) with respect to the left sciatic nerve (1.15×10^{-3} mm^2/s) and a decrease in the fractional anisotropy (FA) values of the right sciatic nerve (0.5) with respect to the left one (0.7). These findings suggest the presence of oedema with increased extracellular space and partial loss of fascicular organisation, compatible with right sciatic neurapraxia. The neurographic reconstruction of the DTI studies (D) (based mainly on the FA threshold value) confirms this asymmetry, with less visualisation of the right sciatic nerve (due to decreased FA values) compared to the left one.

FA values six weeks and even up to six months after the operation, accompanied by a decrease in ADC values.[39]

Interest in the use of advanced DTI neurography techniques in evaluating and monitoring surgical treatment of peripheral nerve disorders has grown in recent years.[31] Surgical techniques such as neurolysis, grafts, transposition or neurotisation can be adequately assessed by DTI neurography, providing additional morphological and functional information about postoperative outcomes. The viability of sutures or grafts, as well as the most frequent surgery-related complications (dehiscence, fibrosis or neuromas) can be studied with these advanced imaging techniques.[40]

The sciatic nerve, one of the most important peripheral nerves due to both its length and its importance in routine clinical practice, has also been assessed using MRN techniques. The presence of intrinsic or extrinsic lesions at the lumbar level or along its pelvic or extra-pelvic trajectory may be caused by compression-related symptoms. There has recently been growing interest in piriformis syndrome and subgluteal sciatic compression as a cause of symptoms related to sciatic neuropathy in patients with no apparent associated disc pathology.[41] The existence of an accessory piriformis muscle or hypertrophy of the piriformis muscle, which occurs in long-distance runners for example, can generate sciatic nerve compression, and would explain the patient's symptoms. This evaluation is usually performed using conventional MRI.[42,43] However, morphology studies frequently fail to show anomalies that would justify the patient's symptoms. This is where diffusion-based neurography techniques can provide additional information on the functional characteristics of the sciatic nerve as it passes through the sciatic foramen.

In these patients, maximum intensity projection (MIP) rendering of diffusion-based MRN images allow radiologists to evaluate the nerve along its entire path, by detecting differences in signal intensity quality of the affected nerve with respect to the contralateral nerve. Furthermore, the nerve will show higher ADC values at the point of compression due to the coexistence of oedema.[44]

The brachial and lumbosacral plexus have also been studied using DWI and DTI neurography sequences.[45,46] DTI studies have shown they can be useful in evaluating traumatic and neoplastic lesions of the brachial and lumbar plexus roots, as well as lesions derived from degenerative disc disease.[47] Regarding lumbar radiculopathy, several studies have evaluated the use of DTI for evaluating lumbar nerve roots in patients with disc pathology based on FA and ADC values, which are significantly lower and higher, respectively, in compressed lumbar roots compared to the contralateral nerve root.[48,49] In the not-too-distant future, this quantitative evaluation may be used to detect functional lumbar root alterations in symptomatic patients, although routine studies do not show clinically relevant findings (Fig. 7).

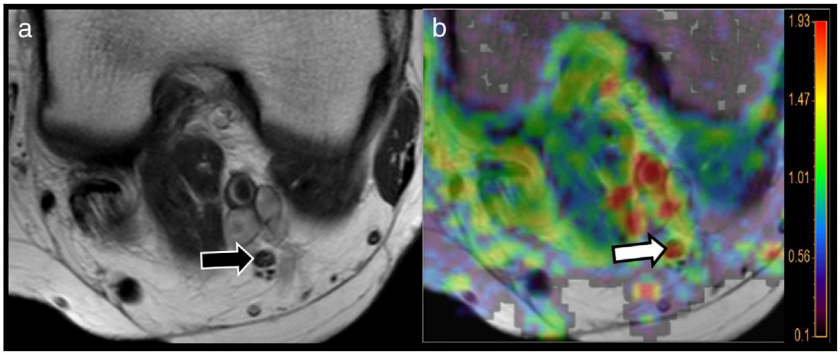

Figure 8 Use of MRI neurography and diffusion tensor imaging (DTI) to evaluate neuropathies. A 64-year-old woman with type 2 diabetes and a 1-year history of paraesthesia in the lower limbs. T2-weighted TSE (A) sequence at the popliteal hollow identified the tibial nerve with preserved morphological features (black arrow). The radial diffusivity (RD) map derived from the MR-neurography study using DTI showed high RD values of the nerve (white arrow points to the red area in the parametric map superimposed on the morphological image) of over 1.9×10^{-3} mm^2/s (see colour scale attached to the figure), suggesting myelin sheath involvement. Bear in mind that one the main mechanisms of diabetic neuropathy is myelin loss secondary to diabetes-induced microvascular damage.

Other peripheral neuropathies

Functional neurography studies can also obtain parameters to help evaluate various types of infectious, inflammatory or metabolic peripheral neuropathies. In these cases, the aim is not to evaluate the integrity of the nerve fascicles, but to complement clinical, analytical and electrophysiological data by determining whether the pathology predominantly affects axonal conduction or the integrity of myelin sheaths. This, for example, will accurately show changes in patients with diabetic neuropathy or chronic inflammatory demyelinating polyneuropathy, and allow clinicians to monitor the evolution of these diseases or evaluate patient response to treatment. In the case of the loss of primary or secondary myelin that occurs in diabetes due to *vasa nervorum* ischaemia, DTI-based neurography studies can not only detect decreases in FA values, but also a more specific parameter, namely, increased radial diffusivity, even in nerves with apparently normal morphological structure[5,50] (Fig. 8).

Tumour pathology

DTI neurography with 3 D visualisation of peripheral nerve pathways has been a breakthrough in the evaluation of nerve tumour pathology. This technology is particularly useful for evaluating the continuity roots or relationship between the lesion under study and the trunks of the plexus or peripheral nerve on which it depends, thus significantly narrowing down the differential diagnosis of such lesions.[51] Secondly, once dependence has been demonstrated, tractography can evaluate the relationship between the nerve fibres and the lesion by showing whether they have been destroyed, displaced or have become disorganised. In the case of neurofibromas, for example, the lesion usually causes a fusiform involve-

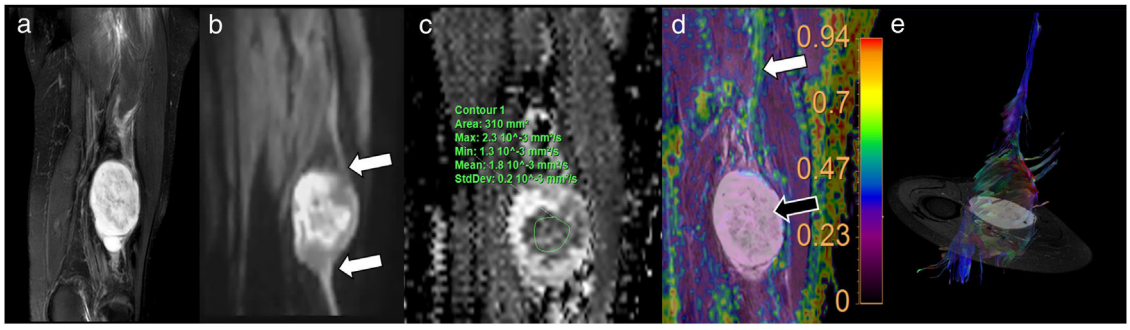

Figure 9 A 57-year-old patient describing a palpable mass in the posterior aspect of the right thigh. The conventional magnetic resonance imaging study using coronal STIR (A) shows a solid fusiform mass impinging on the pathway of the sciatic nerve. Multiplanar reconstruction (MPR) of diffusion-enhanced image (DWI) acquisition (B) confirms the morphological and functional continuity with the mass (white arrows), which shows low apparent diffusion coefficient (ADC) of 1.3×10^{-3} mm^2/s (C). We also performed a diffusion tensor imaging (DTI) study, that showed a marked decrease in fractional anisotropy (FA) values, close to 0 (black arrow), compared to the rest of the nerve, 0.6, in green-yellow range (white arrow) (D) due to absence of fibrillar organisation inside the lesion and eccentric arrangement of the nerve fascicles around the main lesion in the neurological reconstruction (E). A schwannoma was suspected.

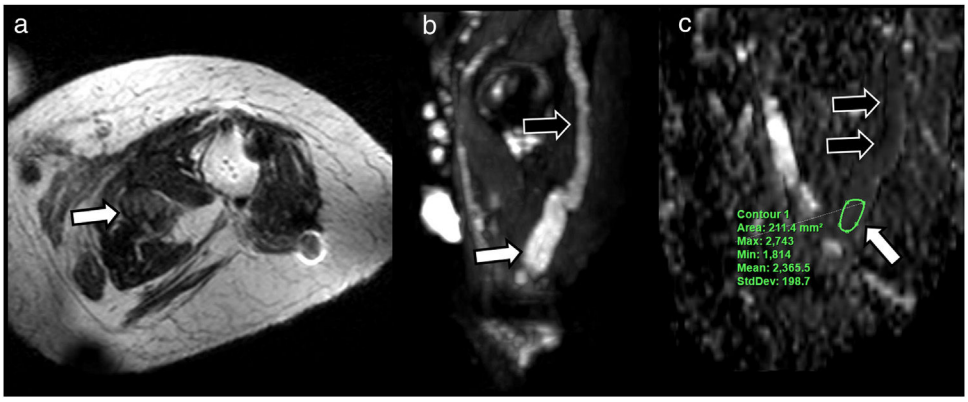

Figure 10 A 33-year-old man with left lower limb amputation due to osteosarcoma. The T2 TSE axial sequence (A) shows a nodular lesion near the surgical bed (white arrow) with heterogeneous signal intensity. MR neurography study with diffusion-enhanced image (DWI) and sagittal multiplanar reconstruction (B) showed anatomical and functional continuity of the sciatic nerve with the lesion (black arrows). The sagittal reconstruction of the ADC map (C) shows values of 1.8×10^{-3} mm^2/s, which was compatible with end-bulb neuroma.

ment of the nerve with diffuse loss of fibres. Schwannoma, however, is usually associated with eccentric displacement of the nerve fascicles[16,52] (Fig. 9). Another type of peripheral nerve lesion that can be studied using these techniques are neuromas-in-continuity or end-bulb neuromas associated with traumatic injury.[53]

As a general rule, malignant tumours have a larger cell population that predominates in the extracellular space, resulting in lower ADC and FA values due to a more disorganised fibre structure (Fig. 10). Benign tumours, however, such as neuromas, neurofibromas or schwannomas, usually show higher ADC values of over 1.1×10^{-3} mm^2/s.[16] Neurography studies can also show invasion of nerve structures by other tumour lesions, or post-radiotherapy changes, such as those that occur in the brachial plexus.[54]

Conclusion

The use of imaging techniques to evaluate peripheral nerve pathology has increased significantly following the development of specific sequences for visualising these structures. Morphological and functional MRI techniques can now be used to reliably characterise the peripheral nerve lesions. DWI and DTI sequences provide additional quantitative information through parameters such as FA or RD, which increase the sensitivity and specificity of MRN studies. However, additional studies are needed to fully validate these techniques.

Authorship

1 Responsible for the integrity of the study: TMN and RB.
2 Study conception: TMN.
3 Study design: TMN.
4 Data collection: TMN and RB.
5 Data analysis and interpretation: TMN and RB.
6 Statistical processing: Not applicable.
7 Literature search: TMN and RB.
8 Drafting of the article: TMN and RB.
9 Critical review of the manuscript with intellectually relevant contributions: TMN and RB.
10 Approval of the final version: TMN and RB.

Conflicts of interest

The authors declare that they have no conflicts of interest.

References

1. Chhabra A, Zhao L, Carrino JA, Trueblood E, Koceski S, Shteriev F, et al. MR Neurography: Advances. Radiol Res Pract. 2013;2013:809568.
2. Wiertel-Krawczuk A, Huber J. Standard neurophysiological studies and motor evoked potentials in evaluation of traumatic brachial plexus injuries – A brief review of the literature. Neurol Neurochir Pol. 2018;52:549–54.
3. Ohana M, Moser T, Moussaouï A, Kremer S, Carlier RY, Liverneaux P, et al. Current and future imaging of the peripheral nervous system. Diagn Interv Imaging. 2014;95:17–26.
4. Stoll G, Wilder-Smith E, Bendszus M. Imaging of the peripheral nervous system. In: Said G, Krarup C, editors. Peripheral Nerve Disorders (Handbook of clinical neurology). Amsterdam: Elsevier B. V.; 2013. p. 37–53.
5. Gasparotti R, Padua L, Briani C, Lauria G. New technologies for the assessment of neuropathies. Nat Rev Neurol. 2017;13:203–16.
6. Kollmer J, Bendszus M, Pham M. MR neurography: Diagnostic Imaging in the PNS. Clin Neuroradiol. 2015;25:283–9.
7. Chhabra A, Flammang A, Padua A, Carrino JA, Andreisek G. Magnetic resonance neurography: technical considerations. Neuroimaging Clin N Am. 2014;24:67–78.
8. Lutz AM, Gold G, Beaulieu C. MR imaging of the brachial plexus. Neuroimaging Clin N Am. 2014;24:91–108.
9. Delaney H, Bencardino J, Rosenberg ZS. Magnetic resonance neurography of the pelvis and lumbosacral plexus. Neuroimaging Clin N Am. 2014;24:127–50.
10. Chhabra A, Andreisek G, Soldatos T, Wang KC, Flammang AJ, Belzberg AJ, et al. MR neurography: Past, present, and future. Am J Roentgenol. 2011;197:583–91.
11. Keller S, Wang ZJ, Golsari A, Kim AC, Kooijman H, Adam G, et al. Feasibility of peripheral nerve MR neurography using diffusion tensor imaging adapted to skeletal muscle disease. Acta Radiol. 2018;59:560–8.

12. de Figueiredo EH, Borgonovi AF, Doring TM. Basic concepts of MR imaging, diffusion MR imaging, and diffusion tensor imaging. Magn Reson Imaging Clin N Am. 2011;19:1–22.
13. Wang X, Harrison C, Mariappan YK, Gopalakrishnan K, Chhabra A, Lenkinski RE, et al. MR Neurography of Brachial Plexus at 3.0 T with Robust Fat and Blood Suppression. Radiology. 2017;283:538–46.
14. Cejas C, Escobar I, Serra M, Barroso F. Neurografía de alta resolución del plexo lumbosacro en resonancia magnética 3 T. Radiologia. 2015;57:22–34.
15. Chhabra A, Subhawong TK, Bizzell C, Flammang A, Soldatos T. 3T MR neurography using three-dimensional diffusion-weighted PSIF: Technical issues and advantages. Skeletal Radiol. 2011;40:1355–60.
16. Ahlawat S, Chhabra A, Blakely J. Magnetic resonance neurography of peripheral nerve tumors and tumorlike conditions. Neuroimaging Clin N Am. 2014;24:171–92.
17. Subhawong TK, Wang KC, Thawait SK, Williams EH, Hashemi SS, MacHado AJ, et al. High resolution imaging of tunnels by magnetic resonance neurography. Skeletal Radiol. 2012;41:15–31.
18. Chhabra A, Chalian M, Soldatos T, Andreisek G, Faridian-Aragh N, Williams E, et al. 3-T high-resolution MR neurography of sciatic neuropathy. Am J Roentgenol. 2012;198:357–64.
19. Chung T, Prasad K, Lloyd TE. Peripheral neuropathy: clinical and electrophysiological considerations. Neuroimaging Clin N Am. 2014;24:49–65.
20. Donovan A, Rosenberg ZS, Cavalcanti CF. MR imaging of entrapment neuropathies of the lower extremity. Part 2. The knee, leg, ankle, and foot. Radiographics. 2010;30:1001–19.
21. Seddon HJ. A Classification of Nerve Injuries. Br Med J. 1942;2:237–9.
22. Sunderland S. Rate of regeneration of sensory nerve fibers. Arch Neurol Psychiatry. 1947;58:1–6.
23. Marquez Neto OR, Leite MS, Freitas T, Mendelovitz P, Villela EA, Kessler IM. The role of magnetic resonance imaging in the evaluation of peripheral nerves following traumatic lesion: where do we stand? Acta Neurochir (Wien). 2017;159:281–90.
24. Schwarz D, Weiler M, Pham M, Heiland S, Bendszus M, Bäumer P. Diagnostic Signs of Motor Neuropathy in MR Neurography: Nerve Lesions and Muscle Denervation. Eur Radiol. 2015;25:1497–503.
25. Takahara T, Hendrikse J, Yamashita T, Mali W, Kwee TC, Imai Y, et al. Diffusion-weighted MR Neurography of the Brachial Plexus: Feasibility Study. Radiology. 2008;249:653–60.
26. Eppenberger P, Andreisek G, Chhabra A. Magnetic resonance neurography: diffusion tensor imaging and future directions. Neuroimaging Clin N Am. 2014;24:245–56.
27. Martín Noguerol T, Barousse R, Socolovsky M, Luna A. Quantitative magnetic resonance (MR) neurography for evaluation of peripheral nerves and plexus injuries. Quant Imaging Med Surg. 2017;7:398–421.
28. Takahara T, Kwee TC, Hendrikse J, Van Cauteren M, Koh D-M, Niwa T, et al. Subtraction of unidirectionally encoded images for suppression of heavily isotropic objects (SUSHI) for selective visualization of peripheral nerves. Neuroradiology. 2011;53:109–16.
29. Kabakci N, Gürses B, Firat Z, Bayram A, Uluğ AM, Kovanlikaya A, et al. Diffusion tensor imaging and tractography of median nerve: normative diffusion values. AJR Am J Roentgenol. 2007;189:923–7.
30. Chhabra A, Williams EH, Subhawong TK, Hashemi S, Soldatos T, Wang KC, et al. MR neurography findings of soleal sling entrapment. AJR Am J Roentgenol. 2011;196:W290–7.
31. Martín Noguerol T, Barousse R, Gómez Cabrera M, Socolovsky M, Bencardino JT, Luna A. Functional MR neurography in evaluation of peripheral nerve trauma and postsurgical assessment. RadioGraphics. 2019;39:427–46.
32. Cejas C, Rollán C, Michelin G, Nogués M. High resolution neurography of the brachial plexus by 3 Tesla magnetic resonance imaging | Neurografía de alta resolución en resonancia magnética 3 Tesla del plexo braquial. Radiologia. 2016;58:88–100.
33. Simon NG, Narvid J, Cage T, Banerjee S, Ralph JW, Engstrom JW, et al. Visualizing axon regeneration after peripheral nerve injury with magnetic resonance tractography. Neurology. 2014;83:1382–4.
34. Grant GA, Goodkin R, Maravilla KR, Kliot M. MR neurography: diagnostic utility in the surgical treatment of peripheral nerve disorders. Neuroimaging Clin N Am. 2004;14:115–33.
35. Heckel A, Weiler M, Xia A, Ruetters M, Pham M, Bendszus M, et al. Peripheral nerve diffusion tensor imaging: Assessment of axon and myelin sheath integrity. PLoS One. 2015;10:e0130833.
36. Georgiev GP, Karabinov V, Kotov G, Iliev A. Medical ultrasound in the evaluation of the carpal tunnel: A critical review. Cureus. 2018;10:e3487.
37. Lindberg PG, Feydy A, Le Viet D, Maier MA, Drapé JL. Diffusion tensor imaging of the median nerve in recurrent carpal tunnel syndrome — initial experience. Eur Radiol. 2013;23:3115–23.
38. Wang CK, Jou IM, Huang HW, Chen PY, Tsai HM, Liu YS, et al. Carpal tunnel syndrome assessed with diffusion tensor imaging: comparison with electrophysiological studies of patients and healthy volunteers. Eur J Radiol. 2012;81:3378–83.
39. Naraghi A, da Gama Lobo L, Menezes R, Khanna M, Sussman M, Anastakis D, et al. Diffusion tensor imaging of the median nerve before and after carpal tunnel release in patients with carpal tunnel syndrome: feasibility study. Skeletal Radiol. 2013;42:1403–12.
40. Chhabra A, Williams EH, Wang KC, Dellon AL, Carrino JA. MR neurography of neuromas related to nerve injury and entrapment with surgical correlation. Am J Neuroradiol. 2010;31:1363–8.
41. Carro LP, Hernando MF, Cerezal L, Navarro IS, Fernandez AA, Castillo AO. Deep gluteal space problems: piriformis syndrome, ischiofemoral impingement and sciatic nerve release. Muscles Ligaments Tendons J. 2016;6:384–96.
42. Varenika V, Lutz AM, Beaulieu CF, Bucknor MD. Detection and prevalence of variant sciatic nerve anatomy in relation to the piriformis muscle on MRI. Skeletal Radiol. 2017;46:751–7.
43. Yang HE, Park JH, Kim S. Usefulness of magnetic resonance neurography for diagnosis of piriformis muscle syndrome and verification of the effect after botulinum toxin type A injection: Two cases. Medicine (Baltimore). 2015;94:e1504.
44. Wada K, Goto T, Takasago T, Hamada D, Sairyo K. Piriformis muscle syndrome with assessment of sciatic nerve using diffusion tensor imaging and tractography: a case report. Skeletal Radiol. 2017;46:1399–404.
45. Wang X, Harrison C, Mariappan YK, Madhuranthakam AJ. MR Neurography of Brachial Plexus at 3.0 T with Robust Fat and Blood Suppression. Radiology. 2017;283:538–46.
46. Tagliafico A, Calabrese M, Puntoni M, Pace D, Baio G, Neumaier CE, et al. Brachial plexus MR imaging: accuracy and reproducibility of DTI-derived measurements and fibre tractography at 3.0-T. Eur Radiol. 2011;21:1764–71.
47. Eguchi Y, Ohtori S, Yamashita M, Yamauchi K, Suzuki M, Orita S, et al. Diffusion-weighted magnetic resonance imaging of symptomatic nerve root of patients with lumbar disk herniation. Neuroradiology. 2011;53:633–41.
48. Balbi V, Budzik J-F, Duhamel A, Bera-Louville A, Le Thuc V, Cotten A. Tractography of lumbar nerve roots: initial results. Eur Radiol. 2011;21:1153–9.
49. Filippi CG, Andrews T, Gonyea JV, Linnell G, Cauley KA. Magnetic resonance diffusion tensor imaging and tractography of the lower spinal cord: application to diastematomyelia and tethered cord. Eur Radiol. 2010;20:2194–9.
50. Tesfaye S, Boulton AJ, Dyck PJ, Freeman R, Horowitz M, Kempler P, et al. Diabetic neuropathies: Update on definitions, diagnostic

criteria, estimation of severity, and treatments. Diabetes Care. 2010;33:2285–93.
51. Chhabra A, Thakkar RS, Andreisek G, Chalian M, Belzberg AJ, Blakeley J, et al. Anatomic MR imaging and functional diffusion tensor imaging of peripheral nerve tumors and tumorlike conditions. AJNR Am J Neuroradiol. 2015;34:802–7.
52. Cortes C, Ramos Y, Restrepo R, Restrepo JA, Grossman JI, Lee EY. Practical magnetic resonance imaging evaluation of peripheral nerves in children: magnetic resonance neurography. Radiol Clin North Am. 2013;51:673–88.
53. Ahlawat S, Belzberg AJ, Montgomery E, Fayad LM. MRI features of peripheral traumatic neuromas. Eur Radiol. 2016;26:1204–12.
54. Fisher S, Wadhwa V, Manthuruthil C, Cheng J, Chhabra A. Clinical impact of magnetic resonance neurography in patients with brachial plexus neuropathies. Br J Radiol. 2016;89, 20160503.